Available online at www.sciencedirect.com
ScienceDirect
Journal of the European Ceramic Society 29 (2009) 3355–3362
www.elsevier.com/locate/jeurceramsoc

Acoustic characterization and microstructure of high zirconia electrofused refractories

C. Patapy, C. Gault, M. Huger, T. Chotard *

Groupe d'Etude des Matériaux Hétérogènes (GEMH), Ecole Nationale Supérieure de Céramique Industrielle, 47 à 73 Avenue Albert Thomas, 87065 Limoges Cedex, France

Received 9 June 2009; received in revised form 6 July 2009; accepted 10 July 2009
Available online 14 August 2009

Abstract

A new line of electrofused refractory materials with a very high content of zirconia (HZ) has been developed to satisfy the needs of new generation manufacturing glass furnaces. Such materials are subjected to severe operating conditions (temperature and corrosion) during their manufacturing and service life. These HZ materials required very high temperature casting and a suitable annealing process to prevent defects and cracks during manufacturing. Therefore, a research program has been launched to build numerical tools able to predict the thermo-mechanical behaviour of these materials during one of the most critical phases of manufacturing: the controlled cooling of the refractory blocks after melting and casting. The efficient development of such a tool requires the knowledge of thermo-mechanical properties of these materials with temperature, in conditions close to that occurring during processing.

In the framework of this approach, the present paper deals with the characterization of elastic properties of two HZ materials, using two mechanical testing devices i.e. a pulse echography technique and a tensile test device. An innovative acoustic emission device is also used to help in identification of microdamage occurrence. The goal of this study is to investigate the microstructure organisation of materials at very fine scale (<100 μm) in order to correlate the obtained results with the macroscopic properties of the material. Characterisations are also performed at intermediate temperature to establish correlations with the manufacturing process.

Keywords: ZrO_2; Refractories; Damage behaviour; Non-destructive evaluation

1. Introduction

Sintered materials have been gradually replaced by electrofused ones in the building of glass furnaces since the second world war. One of the main reasons lies in their ability to have a longer service life.[1] Two parameters convey this quality: the high refractoriness of this kind of material and a particular fully dense microstructure with interlinked phases, which confers good resistance against corrosion by melted glasses. A first generation of electrofused refractories, called AZS (for alumina–zirconia–silica), with a composition around the ternary eutectic one (typically 15 wt.% of silica, 53 wt.% of alumina and 32 wt.% of zirconia), is currently used in most parts of glass furnaces. But since the 1980s, a new generation of electrofused materials, with a high content of monoclinic zirconia (HZ), has been developed to satisfy the need for very low contamination levels for high purity glasses (LCD devices for example). Currently, zirconia is well known to present a very high resistance to corrosion induced by glass and air at high temperature.[2] These materials are also less prone to release polluting compounds in the glass.

The manufacturing process must be rigorously controlled, in particular the cooling rate after melting and casting, in order to limit mechanical stresses induced by important thermal gradients and the martensitic tetragonal–monoclinic transformation of zirconia.[3,4]

The study of the variations with temperature of elastic properties and the characterization of damage by acoustic techniques is thus of a great interest to better understand the evolution of microstructure during this step. In this paper, Young's modulus measurements by an ultrasonic pulse echo technique and an acoustic emission technique have been performed during heat-

* Corresponding author.
E-mail addresses: cedric.patapy@etu.unilim.fr (C. Patapy), christian.gault@unilim.fr (C. Gault), marc.huger@unilim.fr (M. Huger), thierry.chotard@unilim.fr (T. Chotard).

0955-2219/$ – see front matter © 2009 Elsevier Ltd. All rights reserved.
doi:10.1016/j.jeurceramsoc.2009.07.017

ing cycles up to 1500 °C. The main goal is to link mechanical behaviour and microstructure evolution during heat treatments at intermediate temperatures in order to improve the knowledge of mechanisms of stress development and microcracking in the material. Additionally, these measurements, complemented by tensile test experiments, provide thermo-mechanical data which are essential to build efficient numerical tools for the optimization of materials processing conditions.

2. Materials

Two electrofused refractories (referred to as HZ-A and HZ-B) have been manufactured by Saint-Gobain CREE for this study. Both contain 94 wt. % of zirconia and 6 wt. % of glassy phase. The main difference between the two materials is related to the composition of the glassy phase: borosilicate type for HZ-A and alkalisilicate type for HZ-B. An SEM picture of a polished section shows a particular microstructure, which is seen to be polycrystalline with grains surrounded by the glassy phase (Fig. 1).

The material incorporates a three-dimensional inter-linked phase structure organization with dendrites i.e. elongated crystals of zirconia embedded into the glassy phase, as illustrated in Fig. 2 by SEM after HF attack to eliminate the glassy phase, or by 3D X-ray microtomography imaging.[5]

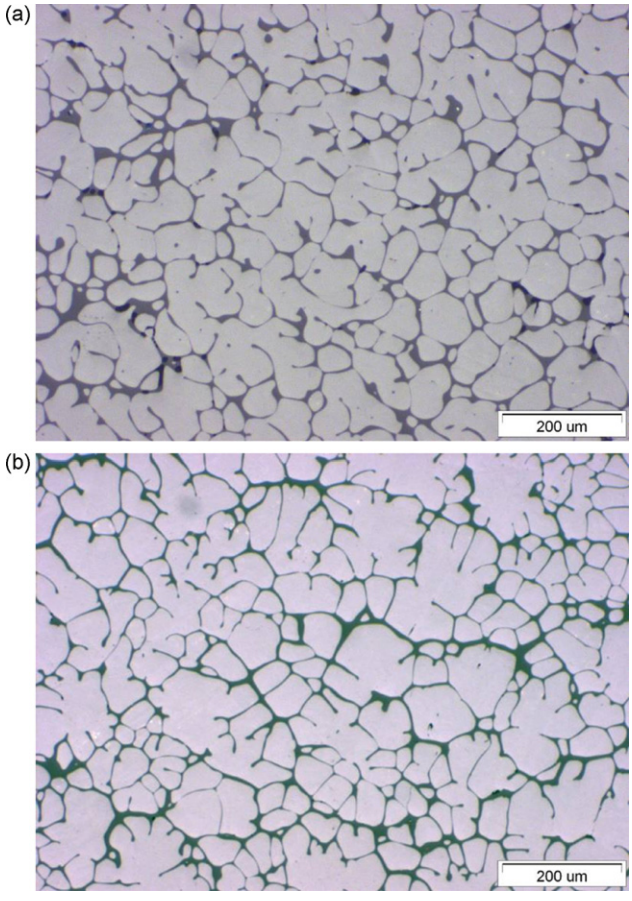

Fig. 1. SEM picture of polished sections of the studied materials: (a) HZ-A and (b) HZ-B.

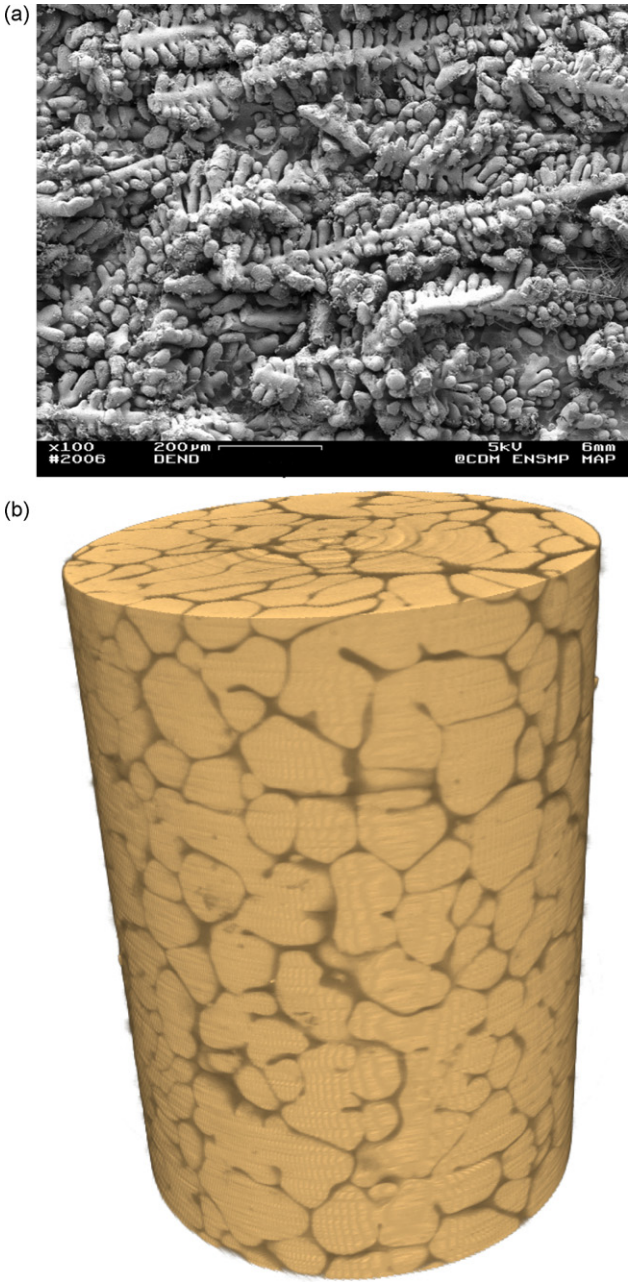

Fig. 2. Micrographies of HZ materials: (a) Zirconia dendrites observed by SEM after an HF attack and (b) X-ray microtomography picture.[5]

The martensitic transformation of zirconia strongly influences the thermo-mechanical behaviour of these materials. The first reason comes from the tetragonal to monoclinic transformation on cooling near 1000 °C, which is well known to generate a 4 vol. % expansion for pure zirconia.[6] The glassy phase within the microstructure is assumed, because of its low viscosity at this temperature, to accommodate internal stresses induced by the anisotropic expansion mismatch between ZrO_2 grains during this transformation. Nevertheless, the transformation of zirconia, combined with TE mismatches between the glassy phase and zirconia, induces microcracking.

Secondly, when cooling, different monoclinic crystallographic equivalent structures can be created from one single

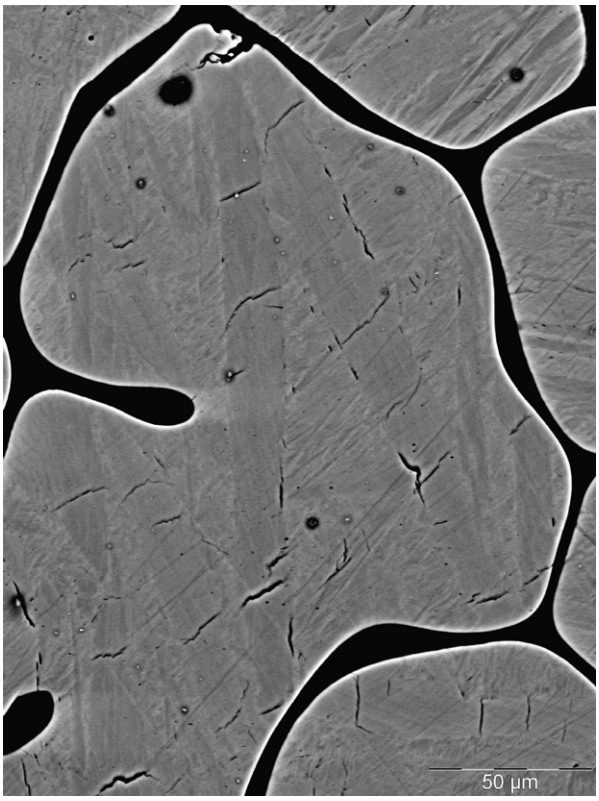

Fig. 3. SEM observation in BSE mode of microcracking patterns on a polished section of HZ-A along twinning directions.

tetragonal crystal.[7] These domains are called variants. The grain is constituted of different variants with different crystallographic orientations since monoclinic zirconia crystals exhibit different thermal expansion coefficients along its crystallographic axes. SEM observations with a specific mechano-chemical polishing procedure using colloidal silica as the last preparation step have been done in BSE mode. They reveal these monoclinic zirconia variants with different twinning directions and the occurrence of microcracks between variants (Fig. 3). Twinning phenomena are widely observed in materials containing zirconia.[8–10] The existence of these multi-orientated variants leads to internal stresses inducing this microcracking development along twinning directions. Such a microstructure is sometimes called a herringbone structure.

Samples for mechanical tests (ultrasonic pulse echo and tensile) and acoustic emission characterization, have been machined in industrial blocks by using diamond tools.

3. Experimental techniques

3.1. High temperature ultrasonic pulse echography

An ultrasonic technique based on the continuous in-situ measurement of the velocity of ultrasonic longitudinal long bar mode has been used to monitor the evolution of Young's modulus in both electrofused materials. The principle is described elsewhere.[11] To achieve satisfactory propagation conditions in this particular ultrasonic mode and taking into account the characteristics of the material, the central frequency of the pulse is 110 kHz and specimens are parallelepipeds of 5.5 mm × 5.5 mm × 100 mm. The measurement of the round trip time, τ, between two successive echoes within the sample makes it possible to calculate the wave velocity and then to obtain the value of the Young's modulus by $E = \rho(2L/\tau)^2$ where L and ρ are sample length and density respectively.

Ultrasonic measurements of Young's modulus have been performed during thermal cycles made at a rate of 5 °C/min for heating and cooling stages and a 1 h isothermal dwell at 1500 °C.

3.2. High temperature acoustic emission technique

Acoustic emission (AE) is defined as "the class of phenomena whereby transient elastic waves are generated by the rapid release of energy from localised sources within the material (or structure) or the transient waves so generated". When a material is subjected to mechanical or thermal stresses, acoustic emission can be generated by a variety of sources such as including crack nucleation and propagation, multiple dislocation slip, twinning, grain boundary sliding, Barkhausen effect (realignment or growth of magnetic domains), phase transformations in alloys, debonding of fibres in composite materials or fracture of inclusions in alloys or twinning are examples.[12–16] It has been used either at the laboratory level or at the industrial scale. Usually, this technique is applied as a non-destructive characterisation technique in order to follow in real-time the evolution of the damage of a material subjected to mechanical loading.[17–19] Others new applications of this technique have been recently developed.[20–23] The originality of this technique developed in the GEMH laboratory lies in the in situ microstructural evolution monitoring at high temperature. Here, the device aims to characterize the damage evolution and the chronology of microstructural changes occurring during thermal cycles.

A wide-band sensor (175 kHz–1 MHz) (PAC MICROPHONE µ80), connected to a preamplifier (EPA 1220A), collects, through an alumina wave-guide, the whole of the signal induced by the elastic waves released within the sample (5.5 mm × 5.5 mm × 25 mm). To avoid parasitic noises from coupling material, a direct contact between the sample and the wave-guide is set. A threshold of 35 dB has been chosen in order to filter background noise. The signal is then amplified and treated by a Mistras acquisition device from Euro Physical Acoustics Company. This system allows the waveform (hit) and the main feature parameters well known in AE study as count, hit, rise time, duration of hit, count to peak, amplitude (in dB) or signal energy, to be recorded. Fig. 4 represents a schematic of the AE system.

AE parameters have been recorded during the same heating–cooling cycles as those used for ultrasonic measurements.

3.3. Tensile tests

Tensile tests have been performed at room temperature with an INSTRON 8862 electro-mechanical universal testing machine. Fig. 5 represents a schematic of the tensile test device

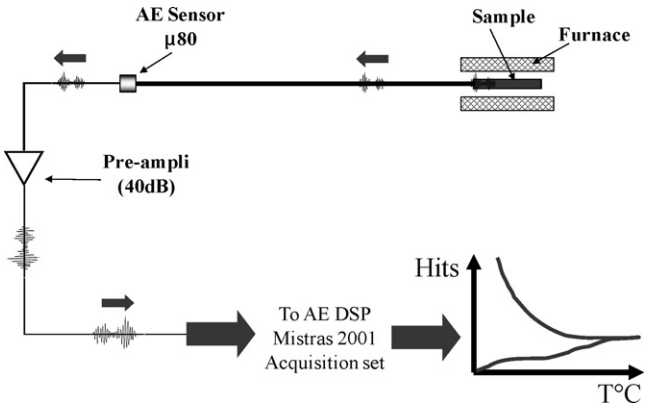

Fig. 4. Schematic of the high temperature acoustic emission-testing device.

which can also work at high temperature up to 1600 °C.[24,25] Strain is evaluated from the variation of a 25 mm gauge length measured by two extensometers equipped by silicon carbide rods which are placed on two opposite faces of the specimen.

The low values of the displacement at rupture exhibited by these materials (3–5 μm) required a good control of the thermal stability of extensometers. Refractory samples are constituted of a cylindrical rod (16 mm in diameter) glued to two metallic parts. The precise final geometry is obtained thanks to a cylindrical machining step of the global assembly.

4. Results and discussion

4.1. Mechanical behaviour at room temperature

Tensile tests have been performed on HZ-A and HZ-B materials at room temperature with a constant stress velocity of 0.02 MPa/s, with intermediate loading–unloading cycles at load levels increasing by step of 0.5 MPa (Fig. 6). It must be noted that the aim of these preliminary experiments is to characterize the tensile behaviour of the materials in order to establish correlations with microstructure and microdamage, not to investigate rupture. Therefore the tests were stopped at a maximum stress of 23 MPa, which roughly corresponds to about 1/2 of the average tensile strength found at room temperature by flexion tests in this type of material.[5]

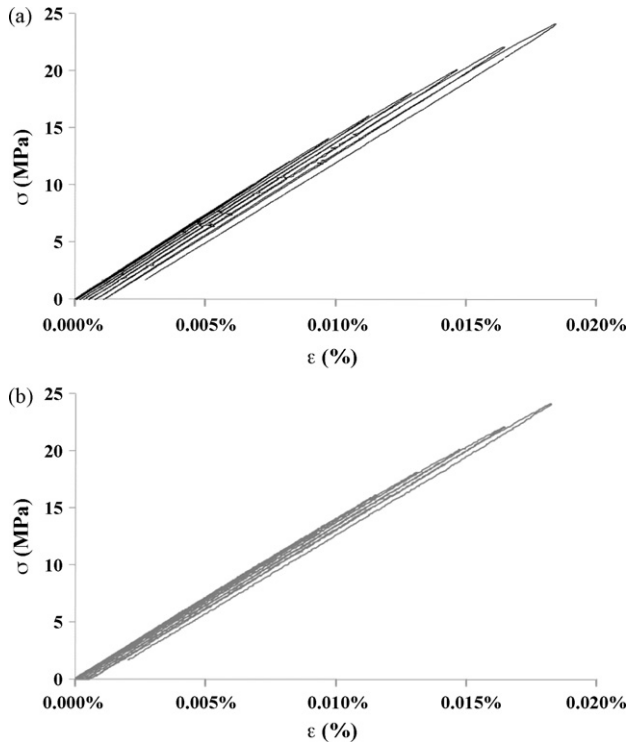

Fig. 6. Tensile stress–strain curves at room temperature with successive loading–unloading cycles at room temperature on both materials: (a) HZ-A and (b) HZ-B.

The two materials display a quasi-linear elastic behaviour. The slight non-linearity and permanent strain after unloading

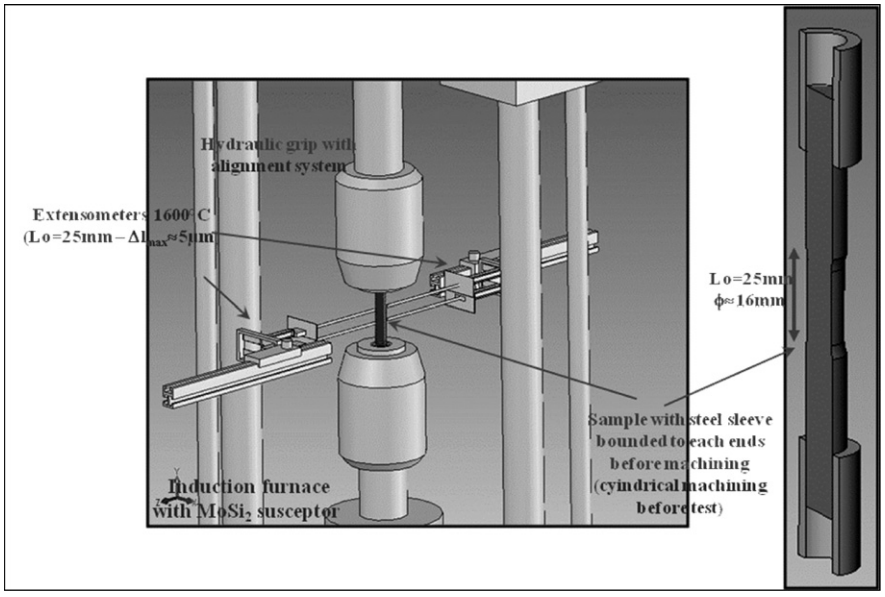

Fig. 5. Schematic of the tensile test device.

Table 1
Young's modulus values obtained by tensile and ultrasonic pulse echo technique tests performed at room temperature for HZ-A and HZ-B materials.

	E (GPa, tensile test)	E (GPa, ultrasonic pulse echography)
HZ-A	149	140
HZ-B	139	132

can be explained by the initial damage of materials after manufacturing. Indeed, successive loading cycles probably involve the opening of microcracks, which pre-exist in the material before test. This phenomenon is more pronounced for HZ-A than for HZ-B. We can notice that initial damage is recovered at operating temperature.

The slope of the first loading step of the stress–strain curve (between 0 and 0.5 MPa,) has been evaluated to determine Young's moduli. The measured values are 149 GPa and 139 GPa for HZ-A and HZ-B respectively. They are compared in Table 1 to Young's moduli determined by the ultrasonic method. The results show that, within the experimental errors and the probable slight dispersion between samples cut in different shapes and different parts of refractory plates, there is a good agreement between the two Young's modulus measurement methods.

For both materials, these values are low in comparison with an estimated theoretical value (180 GPa) of a dense two-phased material based on the intrinsic properties of each phase ($E = 243$ GPa for monoclinic zirconia and $E = 72$ GPa for glassy phase) and using an analytical Hashin–Shtrikman approach.[26] This difference can best be explained by the microdamage which exists in both materials at microscopic scale in their initial state after manufacturing.

4.2. Evolution of elastic modulus and AE during a thermal cycle up to 1500 °C

Ultrasonic measurements of Young's modulus and acoustic emission records have been performed for HZ-A (Fig. 7a) and for HZ-B (Fig. 7b) during thermal cycles up to 1500 °C.

For both materials, three main common features can be noticed:

- The $E = f(T)$ curves exhibit irregular and irreversible aspects, in contrast to the general trend observed in dense ceramics with stable microstructures;
- There are deep modulus effects at the monoclic–tetragonal (M–T) transition temperatures (∼1150 °C on heating for M → T, ∼1000 °C on cooling for T → M);
- Increasing viscous deformation above 1300 °C induces a strong decrease of elasticity and makes ultrasonic measurements impossible above 1400 °C because of a high attenuation.

Considering both Young's modulus and AE curves seven characteristic domains appear: three during heating and four when cooling (Fig. 7).

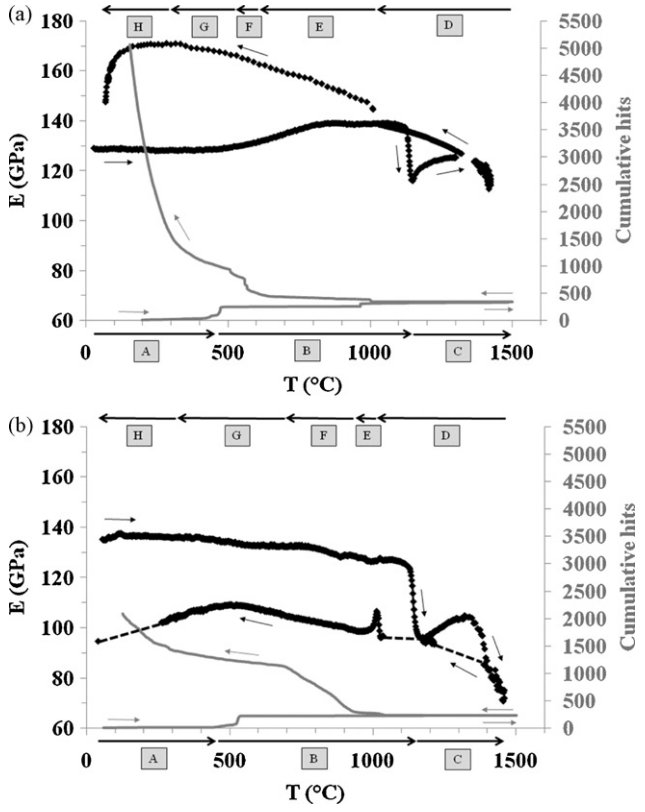

Fig. 7. Young's modulus evolution and cumulative AE vs. temperature during a thermal cycle up to 1500 °C: (a) HZ-A and (b) HZ-B.

- *Domain A*: starting from room temperature E remains quasi-constant, without any acoustic emission up to about 450 °C. At this temperature, the number of hits increases briefly.
- *Domain B*: an increase of E towards a plateau after 850 °C for HZ-A and a regular decrease of E for HZ-B occur without significant AE. At about 1150 °C, the M → T transformation induces a deep transient Young's modulus drop.
- *Domain C*: E increases for both materials up to 1250 °C. As previously mentioned, the materials behaviour becomes visco-plastic above 1300 °C, because of the rapid decrease of viscosity of the glassy phase, which induces a strong decrease of the measured elastic modulus. Note that the subsequent high attenuation of acoustic waves does not allow any record of AE signal in this domain.
- *Domain D*: during the first step of cooling from 1500 °C, and down to the reverse T → M transformation at about 1000 °C, the Young's modulus increases because the materials become stiffer as the viscosity of the glassy phase increases. At this temperature, an increase of AE is observed for both materials. But the evolutions of Young's moduli are different: E increases for HZ-A whereas there is a narrow peak in the case of HZ-B.
- *Domain E*: the Young's modulus slowly increases in parallel with a low acoustic activity from 980 °C to 590 °C for HZ-A and from 980 °C to 920 °C for HZ-B.
- *Domain F*: the regular increase of E remains at the same rate but with a step up of AE for both materials. The temperature

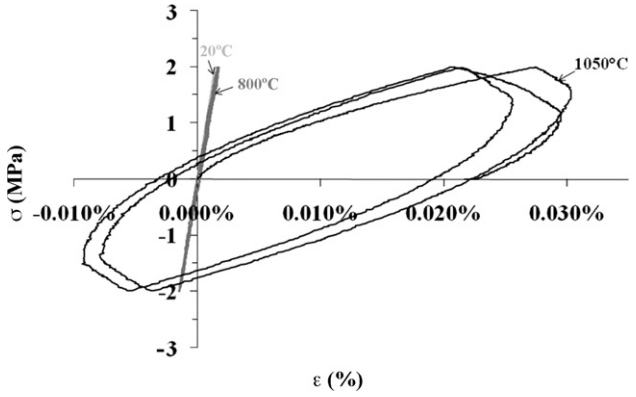

Fig. 8. Tension–compression tests conducted at various temperatures (20 °C, 800 °C and 1050 °C) in HZ-B materials for a stress level of ±2 MPa.

range of this step is of 90 °C for HZ-A whereas it is of 220 °C for HZ-B.

- *Domain G*: a smoothing of acoustic emission corresponds to the beginning of the linearity loss of *E*. Mechanical properties seem to start to be influenced by the damage process. This phenomenon takes place from 500 °C to 300 °C for HZ-A and from 690 °C to 300 °C for HZ-B.
- *Domain H*: from 300 °C to room temperature, an important acoustic activity and a rapid decrease of *E* are observed for both materials.

4.3. Discussion

These results highlight three types of microstructural effects which play major roles in the thermomechanical behaviour during thermal cycles at high temperature. These effects are interdependent and are suspected to be particularly important during the cooling step of processing (annealing).

4.3.1. Glassy phase viscosity

Thermal expansion and Young's modulus measurements versus temperature have been previously performed in samples of synthetic glass with chemical composition close to that of glassy phase in the studied refractories. They showed that the vitreous transition temperature T_g was situated around 800 °C, from which point the elastic properties decrease and dramatically fall down above 1200 °C because of the viscous behaviour of the material. This is illustrated in Fig. 8 where tension–compression cycles under low loading values have been performed at different temperatures (20 °C, 750 °C, 950 °C, 1100 °C). The behaviour is linear elastic up to 750 °C (before T_g of glassy phase), though it is clearly viscous at 1100 °C. The compositions of glassy phases are probably associated with a higher viscosity at given temperature above T_g for HZ-A than for HZ-B. Though the glassy phase proportion being similar in the two materials, a difference of viscosity in the vicinity of M–T zirconia transition can play an important role for relaxation (or not) of internal stresses induced by this transition, in particular when cooling.

Table 2
Young's modulus effects at zirconia transition: $(\Delta E/E)_Z$ predicted from the proper effect of ZrO_2; $(\Delta E/E)_{HZ\text{-}A}$ and $(\Delta E/E)_{HZ\text{-}A}$ values measured on Fig. 7 curves for the two materials.

Temperatures	$(\Delta E/E)_Z$ (%)	$(\Delta E/E)_{HZ\text{-}A}$ (%)	$(\Delta E/E)_{HZ\text{-}B}$ (%)
Heating: 1150 °C	−12.2	−14.3	−21.2
Cooling: 1000 °C	+12.2	+7.1	Peak ± 10.2

4.3.2. $M \leftrightarrow T$ transformation of zirconia

The calculation of Young's modulus versus temperature of an ideal polycrystal of zirconia, byway of an Hashin–Strickman approach[24] reveals a complete symmetric variation during the transformation: $(\Delta E/E)_{M\to T} = -(\Delta E/E)_{T\to M} = -14\%$. The composition of the two materials roughly corresponds to 85 vol.% of ZrO_2. Therefore the expected Young's modulus change $(\Delta E/E)_Z$ coming from the proper effect of phase transition of zirconia can be calculated. The result is listed in Table 2, compared to the characteristics of the modulus effects found in Fig. 7 for the two materials.

The measured effects are somewhat different from the expected ones. In fact they can be considered as the result of two terms:

- on heating at 1150 °C, $(\Delta E/E)_{HZ\text{-}A \text{ or } B} = (\Delta E/E)_{M\to T} + (\Delta E/E)_D$,
- on cooling at 1000 °C, $(\Delta E/E)_{HZ\text{-}A \text{ or } B} = (\Delta E/E)_{T\to M} + (\Delta E/E)_D$,

where $(\Delta E/E)_D$ is due to damage in zirconia and/or intergranular glassy phase, which occurs when internal stresses induced by the volume change associated with the M–T transition, reach critical level. In contrast to the other, this term is always negative, but its amplitude depends on two main factors:

- the ability of the glassy phase to release internal stresses, linked to its viscosity at temperature of M–T transition
- the crack array within zirconia grains which depends on the thermal expansion anisotropy of variants as illustrated in Fig. 3.

Consequently on heating, the deep drop of *E* at 1150 °C is clearly directly caused by the difference of elasticity between monoclinic and tetragonal zirconia, partially enhanced by the effect of microdamage. When cooling from 1500 °C, the T → M transformation at 1000 °C leads to surprising effects: only a slight increase (less than the proper elastic effect of zirconia) for HZ-A and a peak for HZ-B, instead of the expected augmentation. This could be explained by a possible delay between the internal stress relaxation mechanism by microcracking, and the T → M transformation. It must be noted that the level of the AE increase at 1000 °C seems to be more important for HZ-B than for HZ-A which is consistent with this. It must be noted that this mechanism is highly dependent on the thermal history of the material (cooling after melting and casting and subsequent heating at 1500 °C), which influences the microstructure (grain

size, variant texture) and then the conditions of development of internal stresses at the transformation.

4.3.3. Microdamage evolution

It is more convenient to discuss microdamage evolution, starting from the high temperature state (1500 °C). Indeed, at this temperature, the material is constituted of stable tetragonal zirconia crystals surrounded by a very low viscosity glassy phase. Therefore it can be assumed to be free of internal stress and with a minimum of damage, because of intergranular crack healing by the glassy phase. This is also the stable state of the material at the application temperature in a glass furnace. As previously noted, ultrasonic measurements are difficult above 1300 °C because of the high ultrasonic attenuation associated with the viscous behaviour. Then a recovery of the signal is progressively observed on cooling corresponding to the stiffening of the material down to 1000 °C where the T → M transition occurs.

As discussed, this transition is accompanied by an important internal stress field:

- in zirconia particles, caused by thermal expansion mismatches between variants,
- around zirconia particles, because of the expansion associated to the transition.

It is probable that the second phenomenon leads to shortly delayed microcracking after the T → M transition, though the first one occurs on cooling at critical temperatures corresponding to thermal stress values sufficient to induce cracking inside zirconia grains at microscopic scale. Temperature domains F and H, where AE is particularly intense, could be linked to such mechanisms. Additionally, when cooling down to room temperature, a decrease of Young's modulus due to damage is observed, but it appears that the Young's modulus of HZ-B begins to drop earlier in temperature than the one of HZ-A. The zirconia variants reorganization after the T → M transformation may influence the difference of behaviour between the two materials. Anyway, further work will be necessary to establish quantitative correlations between the damage mechanisms and microstructural parameters of the materials. Microcracks resulting from damage processes can be observed by SEM after a thermal cycle at 1500 °C (Fig. 9).

When heating from room temperature, Young's modulus regularly decreases and no noticeable AE signal occurs up to about 500–600 °C (domain A) in both materials. This denotes a microstructure stable versus temperature. At the end of domain A, a deep small increase of AE activity is observed which could be due to a reorganization of microdamage inside the zirconia skeleton. Anyway, the mechanism responsible for this effect is not yet clear. After that (domain B), thermal crack closure tends to stiffen the material, though the materials become softer according to the decrease of viscosity of the glassy phase above T_g ($\gtrsim$800 °C). The consequence is a very small increase of E followed by a plateau for HZ-A and a quasi-regular decrease for HZ-B.

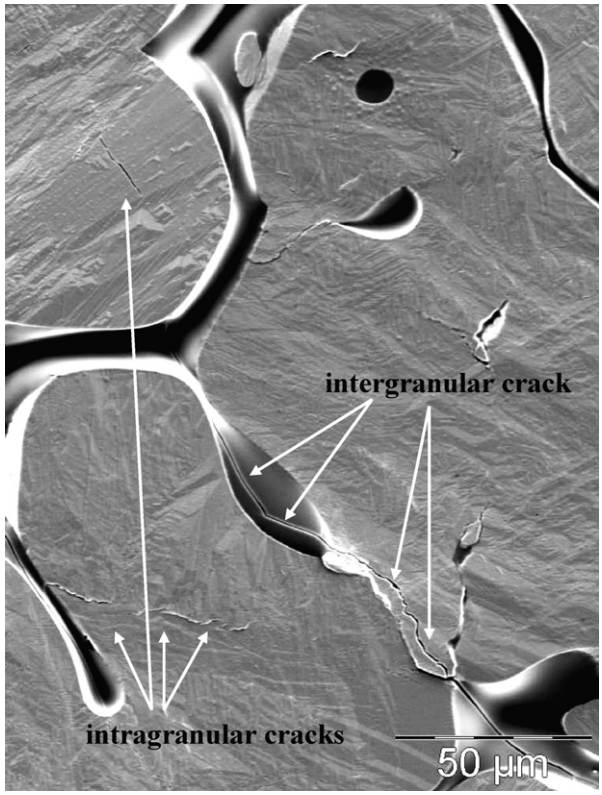

Fig. 9. Microstructure observed after a heat treatment at 1500 °C on a prepolished section of HZ-A material.

At 1150 °C, the effect of M → T transition of zirconia has been previously discussed. Note that it is accompanied by a damage due to volume contraction, which is then healed by the low viscosity glassy phase, inducing a stiffening during the first part of domain C. Above 1300 °C, the two materials exhibit a strong visco-plastic behaviour and it can be supposed that at 1500 °C, microdamage is quite reabsorbed.

5. Conclusion

Thermo-mechanical properties of two electrofused materials with differences related to composition of the glassy phase have been investigated both by ultrasonic measurements and by tensile tests. Both tensile and ultrasonic techniques show good correlation in Young's modulus evaluation at room temperature. HZ-A and HZ-B show a quasi-linear elastic behaviour. The rather low values of Young's modulus for such fully dense materials show that high zirconia electrofused refractories are microdamaged after processing. Even if it does not affect performance of materials at operating temperature for glass manufacturing because microcracks are totally recovered, it makes it possible to understand which microstructure mechanisms are involved during heat treatment. A parallel, between ultrasonic echography and acoustic emission performed at high temperature, links the mechanical behaviour to microstructure changes.

Microstructure and thermo-mechanical evolutions are highlighted in this paper. Firstly, the possible role of the glassy

phase and its ability to relax stresses through the viscosity is underlined. Then, phenomena occurring during the martensitic transformation of zirconia are explained. More precisely, as crystallographic structures (monoclinic and tetragonal) of ZrO_2 do not have the same elastic properties, it appears logical to see a gap in Young's modulus value at the transition temperature. But the Hashin–Shtrickman approach predicts a perfect reversibility of E evolution during $M \rightarrow T$ and $T \rightarrow M$. Asymmetry of $(\Delta E/E)$ observed by pulse echo technique is thus a consequence of some microdamage which occurs more visibly during cooling. This microdamage evolves during cooling and is predominantly governed by anisotropy of zirconia variants above the glassy phase transition temperature (T_g) and by thermal expansion mismatches between the glassy phase and zirconia grains below. Further work is now undertaken, on the one hand in order to better understand these crystallographic orientations, by investigations using XRD and neutron scattering, on the other hand to verify the influence of a stress field upon the variant formation by using acoustic emission associated with thermal expansion analysis during successive thermal cycles around the M–T transformation.

Acknowledgements

Authors are greatly thankful to Saint-Gobain CREE, industrial partner in the NOREV program, for supplying the materials and to the French National Research Agency (ANR) for its financial support.

References

1. Begley, E. R. and Herndon PO, Zirconia–alumina–silica refractories. In *High temperature oxides: refractory glasses, glass-ceramics, and ceramics*, *vol. 5-IV*, ed. A. M. Alper. Academic Press, New York and London, 1971, pp. 185–208.
2. Ishino, T., Fusion cast refractories. *Refractories handbook*. The Technical Association of Refractories, Tokyo, Japan, 1998, pp. 201–209.
3. Bardhan, P. and Mcnally, R. N., Fusion casting and crystallisation of high temperature materials. *J. Mater. Sci.*, 1980, **15**, 2409–2427.
4. Shaw, K., *Refractories and their uses*. Applied Science Publishers LTD, London, 1972.
5. Lataste, E., *Comportement mécanique et endommagement de réfractaires électrofondus sous sollicitation thermomécanique*. PhD, INSA Lyon, France, 2005.
6. Yeugo Fogaing, E., *Caractérisation à haute température des propriétés d'élasticité de réfractaires électrofondus et de bétons réfractaires*. PhD, University of Limoges, France, 2006.
7. Kisi, E. H. and Howard, C. J., In *Crystal structures of zirconia phases and their inter-relation, zirconia engineering ceramics*. Edition Erich Kisi 1998, pp. 1–10.
8. Arshad Choudhry, M. and Crocker, A. G., Theory of twinning and transformation modes in zirconia. *Science and Technology of Zirconia II (Advances in Ceramics)*, *vol. 12*. The American Ceramic Society, Stuttgart, 1984, pp. 46–53.
9. First, R. C. and Heuer, A. H., Deformation by moving interfaces (deformation twinning) in monoclinic zirconia (Baddeleyite). *J. Struct. Geol.*, 1993, **15**, 1241–1247.
10. Simha, N. K., Twin and habit plane microstructures due to the tetragonal to monoclinic transformation of zirconia. *J. Mech. Phys. Solids*, 1997, **45**, 261–292.
11. Huger, M., Fargeot, D. and Gault, C., High-temperature measurement of ultrasonic wave velocity in refractory material. *High Temp. High Pres.*, 2002, **34**, 193–201.
12. Hamstad, M. A., Thompson, P. M. and Young, R. D., Flaw growth in alumina studied by acoustic emission. *J. Acoust. Emis.*, 1987, **6**, 93–97.
13. Bakuckas, J. G., Prosser, W. H. and Johnson, W. S., Monitoring damage growth in titanium matrix composites using acoustic emission. *J. Comp. Mater.*, 1994, **28**, 305–328.
14. Berkovits, A. and Fang, D., Study of fatigue crack characteristics by acoustic emission. *Eng. Fract. Mech.*, 1995, **51**, 401–416.
15. Havlicek, F. and Crha, J., Acoustic emission monitoring during solidification processes. *J. Acoust. Emis.*, 1999, **17**, 3–4.
16. Coddet, C., Chretien, J. F. and Beranger, G., Investigation on the fracture mechanism of oxide layers growing on titanium by acoustic emission. *Titanium Titanium Alloys: Sci. Technol. Aspects*, 1982, **2**, 1097–1105.
17. Barré, S. and Benzeggagh, M. L., On the use of acoustic emission to investigate damage mechanisms in glass-fibre-reinforced polypropylene. *Comp. Sci. Technol.*, 1994, **52**, 369–376.
18. Suzuki, H., Takemoto, M. and Ono, K., The fracture dynamics in a dissipative glass fibber/epoxy model composite with AE source simulation analysis. *J. Acoust. Emis.*, 1996, **14**, 35–50.
19. Pauchard, V., Brochado, S., Chateauminois, A., Campion, H. and Grosjean, F., Measurement of sub-critical crack-growth rates in glass fibbers by means of acoustic emission. *J. Mater. Sci. Lett.*, 2000, **19**, 2141–2143.
20. Chotard, T., Smith, A., Rotureau, D., Fargeot, D. and Gault, C., Acoustic emission characterisation of calcium aluminate cement hydration at an early stage. *J. Eur. Ceram. Soc.*, 2003, **23**, 387–398.
21. Chotard, T., Quet, A., Ersen, A. and Smith, A., Application of the acoustic emission technique to characterise liquid transfer in a porous ceramic during drying. *J. Eur. Ceram. Soc.*, 2006, **26**, 1075–1084.
22. Chotard, T., Soro, J., Lemercier, H., Huger, M. and Gault, C., High temperature characterization of Cordierite-Mullite refractory by ultrasonic means. *J. Eur. Ceram. Soc.*, 2008, **28**, 2129–2135.
23. Briche, G., Tessier-Doyen, N., Huger, M. and Chotard, T., Investigation of damage behaviour of refractory model materials at high temperature by combined pulse echography and acoustic emission techniques. . *Eur. Ceram. Soc.*, 2008, **28**, 2835–2843.
24. Ghassemi Kakroudi, M., *Comportement thermomécanique en traction de bétons réfractaires: influence de la nature des agrégats et de l'histoire thermique*. PhD, University of Limoges, France, 2007.
25. Ghassemi Kakroudi, M., Yeugo Fogaing, E., Huger, M., Chotard, T. and Gault, C., Effect of thermal treatment on damage mechanical behaviour of refractory castables: comparison between bauxite and andalusite aggregates. *J. Eur. Ceram. Soc.*, 2008, **28**, 2471–2478.
26. Yeugo Fogaing, E., Lorgouilloux, Y., Huger, M. and Gault, C., Young's modulus of zirconia at high temperature. *J. Mater. Sci. Lett.*, 2006, **41**, 7663–7666.